doi: 10.18720/MCE.74.12

The stress-strain state of ribbed shell structures

Напряженно-деформированное состояние ребристых оболочечных конструкций

V.V. Karpov,
St. Petersburg State University of Architecture and Civil Engineering, St. Petersburg, Russia
O.V. Ignat'ev,
Peoples Friendship University of Russia (RUDN University), Moscow, Russia
A.A. Semenov,
St. Petersburg State University of Architecture and Civil Engineering, St. Petersburg, Russia

Д-р техн. наук, профессор В.В. Карпов,
Санкт-Петербургский государственный архитектурно-строительный университет, г. Санкт-Петербург, Россия,
д-р техн. наук, заведующий кафедрой О.В. Игнатьев,
Российский университет дружбы народов, г. Москва, Россия,
канд. техн. наук, доцент А.А. Семенов,
Санкт-Петербургский государственный архитектурно-строительный университет, г. Санкт-Петербург, Россия

Key words: shells; stiffened shells; stiffening ribs; stresses; deformation

Ключевые слова: оболочки; подкрепленные оболочки; ребра жесткости; напряжения; деформирование

Abstract. The paper presents an analysis of the stress-strain state of shallow shell structures of double curvature, reinforced from the concave side by a various number of stiffeners. Mindlin–Reissner shell deformation theory is used, which accounts for geometrical nonlinearity and transverse shears, as well as for discrete introduction of stiffeners with contact between the stiffener and the shell along the strip. The mathematical model is written in the form of a functional of full potential deformation energy. The algorithm of the analysis is based on the application of the Ritz method to the functional, which is used for reducing the problem to a system of nonlinear algebraic equations. The resulting system is solved by the parameter continuation method. Structural variations that are considered in the paper are fastened with fixed-pin joints along the contour and are subject to external uniformly distributed transverse loading. The values of stresses, forces, and moments in the stiffeners and in the shell skin are obtained and analyzed. Specific features of their distribution are revealed. All values are given in dimensionless parameters. It is shown that accounting for the contact of the stiffener with the shell skin along the strip allows one to investigate the stress-strain state in the stiffeners, which are not possible using delta functions with the introduction of stiffeners along the line.

Аннотация. В работе проводится анализ напряженно-деформированного состояния пологих оболочечных конструкций двоякой кривизны, подкрепленных со стороны вогнутости различным числом ребер. Используется теория деформирования оболочек Миндлина–Рейснера, учитывающая геометрическую нелинейность, поперечные сдвиги, а также дискретное введение ребер жесткости с контактом ребра и обшивки по полосе. Математическая модель записана в виде функционала полной потенциальной энергии деформации. Алгоритм расчета основан на применении к функционалу метода Ритца для сведения задачи к системе нелинейных алгебраических уравнений. Полученная система решается методом продолжения решения по параметру. Рассматриваемые варианты конструкций шарнирно неподвижно закреплены по контуру и находятся под действием внешней равномерно распределенной поперечной нагрузки. Анализируются полученные данные о значениях напряжений, усилий и моментов в ребрах жесткости и в обшивке. Выявлены особенности их распределения. Значения приведены в безразмерных параметрах. Показано, что учет контакта ребра с обшивкой по полосе позволяет исследовать напряженно-деформированное состояние в ребрах, что невозможно при введении ребер по линии с помощью дельта-функций.

Карпов В.В., Игнатьев О.В., Семенов А.А. Напряженно-деформированное состояние ребристых оболочечных конструкций // Инженерно-строительный журнал. 2017. № 6(74). С. 147-160.

Introduction

The study of the behavior of shell structures is essential for different sectors of industry [1–4], including Civil Engineering [5–6]. For thin-walled shells, it is important to account for the reinforcement with stiffeners [7–35], which make it possible to significantly increase the critical load value, redistribute hazardous stresses, and thus increase the robustness of the structure.

Most of the stability studies of reinforced shells were carried out for closed cylindrical shells [10, 11, 17, 20, 21, 29–31], because such structures are the most widely used in practice. In addition, due to their symmetry, they can be analyzed using simplified models (as an axisymmetric problem).

According to the type of external action, structures under axial compression are more frequently investigated [11–22, 27–29, 32], whereas structures under uniformly distributed transverse loading are studied less often [15–18, 26, 27].

Stability of shells under static loading is considered in [16–24], and the vibrations of such structures in [7, 8, 13–15, 32]. Optimization issues of reinforced shells for solving specific practical problems were discussed in [26–30].

In most cases the stiffeners are located on the side of the concavity of the shell, but the cases where the stiffeners are located on the external side of the shell are also of interest [17, 18, 28, 31].

The finite element method for calculating reinforced thin-walled shells was used in [4, 7, 8, 11, 17, 20, 25, 26, 34, 35].

In most studies it is assumed that stiffeners interact with the shell skin along the line: thus, for example, A.I. Lurie [36] and V.Z. Vlasov [37] considered the stiffeners as Kirchhoff–Klebsch bars, where the locations of stiffeners were defined with the aid of delta functions. With this approach, it is assumed [38] that the effect of shell-reinforcing stiffeners on the shear and torsion of the median surface of the shell skin can be neglected, and deformation of reinforcements is described by the relations of a linear stress state without accounting for their interaction.

The most accurate approach is when the contact between the stiffener and the shell skin occurs along the strip [39]. Also, for reinforced shells, it is essential to account for transverse shears [40].

The purpose of this paper is to analyze the stress-strain state of stiffened shell structures and to identify the features of their deformation process.

The objective of the study is to perform a computational experiment to determine the stress-strain state of shallow shells of rectangular base with a varying number of shell-reinforcing stiffeners.

Methods

Let us consider shallow isotropic shell structures of double curvature, of square base (Figure 1), with fixed-pin joints along the contour and subjected to external uniformly distributed transverse loading q. The load is oriented along the normal to the median surface. The shell is reinforced from the concave side by an orthogonal grid of stiffeners, parallel to the coordinate lines.

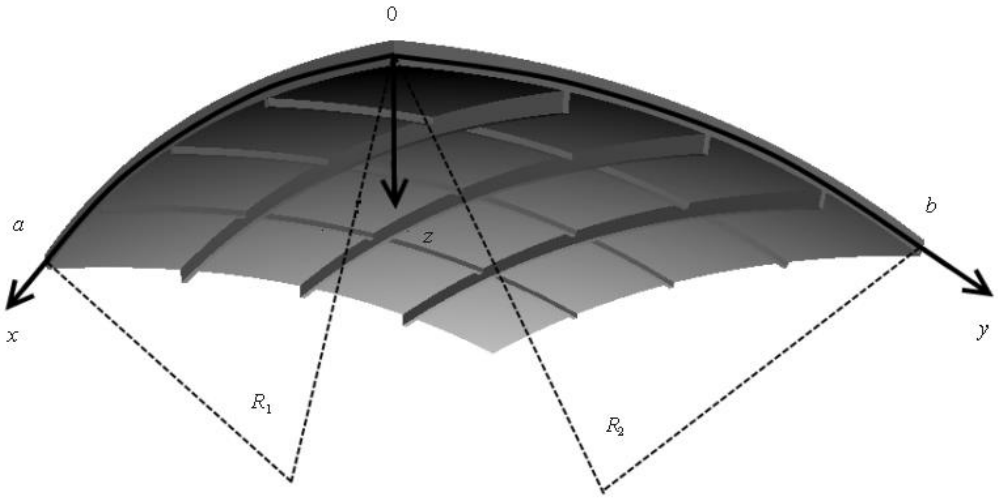

Figure 1. Schematic representation of a shallow shell structure of double curvature, of square base

Karpov V.V., Ignat'ev O.V., Semenov A.A. The stress-strain state of ribbed shell structures. *Magazine of Civil Engineering*. 2017. No. 6. Pp. 147–160. doi: 10.18720/MCE.74.12.

Mathematical model

The mathematical model of deformation of such structures is constructed from three groups of relations: geometric (associating displacements and strains), physical (associating stresses and strains), and the functional of the total potential deformation energy.

Let us consider a geometrically nonlinear version of the model, which also takes into account transverse shears (the Mindlin–Reissner model), and the possibility of discrete introduction of stiffeners, taking into account the contact of the stiffener and the shell skin along the strip and accounting for the shear and torsional rigidity of the stiffeners. In this case, the unknown functions are three displacement functions $U = U(x, y)$, $V = V(x, y)$, and $W = W(x, y)$ and two functions of the angles of rotation of the normal, $\Psi_x = \Psi_x(x, y)$, and $\Psi_y = \Psi_y(x, y)$; and the geometric relations will have the form:

$$\varepsilon_x = \frac{\partial U}{\partial x} - k_x W + \frac{1}{2}\theta_1^2, \ \varepsilon_y = \frac{\partial V}{\partial y} - k_y W + \frac{1}{2}\theta_2^2, \ \gamma_{xy} = \frac{\partial V}{\partial x} + \frac{\partial U}{\partial y} + \theta_1\theta_2,$$
$$\chi_1 = \frac{\partial \Psi_x}{\partial x}, \ \chi_2 = \frac{\partial \Psi_y}{\partial y}, \ 2\chi_{12} = \frac{\partial \Psi_y}{\partial x} + \frac{\partial \Psi_x}{\partial y}, \tag{1}$$

where $\varepsilon_x, \varepsilon_y$ are axial strains along the x and y coordinates of the median surface; γ_{xy} is the shear strain in the xOy plane; $\chi_1, \chi_2, \chi_{12}$ are functions of change of curvatures and torsion; $k_x = 1/R_1, k_y = 1/R_2$ are primary curvatures of the shell along the x and y axes; R_1, R_2 are the principal radii of curvature; and

$$\theta_1 = -\frac{\partial W}{\partial x}, \quad \theta_2 = -\frac{\partial W}{\partial y}. \tag{2}$$

The physical relations for linearly elastic deformation of an isotropic material under a plane stress state will have the form

$$\sigma_x = \frac{E}{1-\mu^2}\left[\varepsilon_x + \mu\varepsilon_y + z(\chi_1 + \mu\chi_2)\right]; \ \sigma_y = \frac{E}{1-\mu^2}\left[\varepsilon_y + \mu\varepsilon_x + z(\chi_2 + \mu\chi_1)\right];$$
$$\tau_{xy} = G_{12}\left[\gamma_{xy} + 2z\chi_{12}\right], \tag{3}$$

where E is the elastic modulus of an isotropic material; μ is the Poisson's ratio; and G_{12} is the shear modulus.

Expressions for forces and moments are separated into components acting in the shell skin (index 0), and in the stiffeners (index R). Consequently, we have

$$N_x = N_x^0 + N_x^R, \quad N_y = N_y^0 + N_y^R, \quad N_{xy} = N_{xy}^0 + N_{xy}^R, \quad N_{yx} = N_{yx}^0 + N_{yx}^R,$$
$$M_x = M_x^0 + M_x^R, \quad M_y = M_y^0 + M_y^R, \quad M_{xy} = M_{xy}^0 + M_{xy}^R, \quad M_{yx} = M_{yx}^0 + M_{yx}^R, \tag{4}$$
$$Q_x = Q_x^0 + Q_x^R, \quad Q_y = Q_y^0 + Q_y^R.$$

If the stiffeners are introduced discretely, then in the expressions (4) one should take [35]

$$N_x^0 = G_1 h(\varepsilon_x + \mu\varepsilon_y), \quad N_y^0 = G_1 h(\varepsilon_y + \mu\varepsilon_x), \quad N_{xy}^0 = N_{yx}^0 = G_{12} h\gamma_{xy},$$
$$M_x^0 = G_1 \frac{h^3}{12}(\chi_1 + \mu\chi_2), \quad M_y^0 = G_1 \frac{h^3}{12}(\chi_2 + \mu\chi_1), \quad M_{xy}^0 = M_{yx}^0 = 2G_{12}\frac{h^3}{12}\chi_{12},$$
$$Q_x^0 = G_{13} kh(\Psi_x - \theta_1), \qquad Q_y^0 = G_{23} kh(\Psi_y - \theta_2),$$
$$N_x^R = G_1\left[F(\varepsilon_x + \mu\varepsilon_y) + S(\chi_1 + \mu\chi_2)\right], \quad N_y^R = G_1\left[F(\varepsilon_y + \mu\varepsilon_x) + S(\chi_2 + \mu\chi_1)\right],$$
$$N_{xy}^R = N_{yx}^R = G_{12}\left[F\gamma_{xy} + 2S\chi_{12}\right], \tag{5}$$

Карпов В.В., Игнатьев О.В., Семенов А.А. Напряженно-деформированное состояние ребристых оболочечных конструкций // Инженерно-строительный журнал. 2017. № 6(74). С. 147-160.

$$M_x^R = G_1\left[S\left(\varepsilon_x + \mu\varepsilon_y\right) + J\left(\chi_1 + \mu\chi_2\right)\right], \quad M_y^R = G_1\left[S\left(\varepsilon_y + \mu\varepsilon_x\right) + J\left(\chi_2 + \mu\chi_1\right)\right],$$
$$M_{xy}^R = M_{yx}^R = G_{12}\left[S\gamma_{xy} + 2J\chi_{12}\right],$$
$$Q_x^R = G_{13}kF\left(\Psi_x - \theta_1\right), \qquad Q_y^R = G_{23}kF\left(\Psi_y - \theta_2\right), \; G_1 = \frac{E}{1-\mu^2}.$$

Here h is the thickness of the shell skin; F, S, and J are the area of the cross-sectional or longitudinal section of the stiffener per unit length of the cross-section; the static moment of the area; and the moment of inertia of this cross-section. In the discrete approach, it is taken into account that the contact of the stiffener with the shell skin occurs along the strip, the shear and torsional rigidity of the stiffeners are taken into account, and then these characteristics are calculated as follows [41]:

$$F = \sum_{j=1}^{m} F^j \delta\left(x - x_j\right) + \sum_{i=1}^{n} F^i \delta\left(y - y_i\right) - \sum_{i=1}^{n}\sum_{j=1}^{m} F^{ij} \delta\left(x - x_j\right)\delta\left(y - y_i\right);$$
$$S = \sum_{j=1}^{m} S^j \delta\left(x - x_j\right) + \sum_{i=1}^{n} S^i \delta\left(y - y_i\right) - \sum_{i=1}^{n}\sum_{j=1}^{m} S^{ij} \delta\left(x - x_j\right)\delta\left(y - y_i\right); \tag{6}$$
$$J = \sum_{j=1}^{m} J^j \delta\left(x - x_j\right) + \sum_{i=1}^{n} J^i \delta\left(y - y_i\right) - \sum_{i=1}^{n}\sum_{j=1}^{m} J^{ij} \delta\left(x - x_j\right)\delta\left(y - y_i\right),$$

where

$$F^i = h^i, \; F^j = h^j, F^{ij} = h^{ij}, S^i = h^i\left(h + h^i\right)/2, S^j = h^j\left(h + h^j\right)/2, S^{ij} = h^{ij}\left(h + h^{ij}\right)/2,$$
$$J^i = 0.25h^2h^i + 0.5h\left(h^i\right)^2 + \frac{1}{3}\left(h^i\right)^3, \tag{7}$$
$$J^j = 0.25h^2h^j + 0.5h\left(h^j\right)^2 + \frac{1}{3}\left(h^j\right)^3, \quad J^{ij} = 0.25h^2h^{ij} + 0.5h\left(h^{ij}\right)^2 + \frac{1}{3}\left(h^{ij}\right)^3.$$

Here h^i, h^j are the height of the stiffener; indices i and j indicate the order number of the stiffener located parallel to the x and y axes, respectively; n, m are the number of stiffeners; $h^{ij} = \min\left\{h^i, h^j\right\}$; and $\delta\left(x - x_j\right)$, $\delta\left(y - y_j\right)$ are unit bar graph functions equal to 1 in places where stiffeners are connected, which are equal to the difference of two unit functions:

$$\delta\left(x - x_j\right) = U\left(x - a_j\right) - U\left(x - b_j\right), \quad \delta\left(y - y_i\right) = U\left(y - c_i\right) - U\left(y - d_i\right). \tag{8}$$

Moreover, $a_j = x_j - r_j/2, \quad b_j = x_j + r_j/2, \quad c_i = y_i - r_i/2, \quad d_i = y_i + r_i/2$, where r_i, r_j are the width of the stiffener; and indices i and j indicate the order number of the stiffeners located parallel to the x and y axes, respectively.

The total potential deformation energy of a shallow shell of double curvature can be written with the aid of a functional E_p that represents the difference of the potential deformation energy of the system and the work of external forces:

$$E_p = \frac{1}{2}\int_0^a\int_0^b \Big\{ N_x\varepsilon_x + N_y\varepsilon_y + \frac{1}{2}\left(N_{xy} + N_{yx}\right)\gamma_{xy} + M_x\chi_1 + M_y\chi_2 + \left(M_{xy} + M_{yx}\right)\chi_{12} + \tag{9}$$
$$+ Q_x\left(\Psi_x - \theta_1\right) + Q_y\left(\Psi_y - \theta_2\right) - 2qW \Big\} dxdy.$$

Representing this functional as the sum of two functionals, individually corresponding to the shell skin and the stiffeners, we obtain

$$E_p = E_p^0 + E_p^R, \tag{10}$$

where [41]

$$E_p^0 = \frac{1}{2}\int_0^a\int_0^b \Big\{ N_x^0\varepsilon_x + N_y^0\varepsilon_y + \frac{1}{2}\left(N_{xy}^0 + N_{yx}^0\right)\gamma_{xy} + M_x^0\chi_1 + M_y^0\chi_2 + \left(M_{xy}^0 + M_{yx}^0\right)\chi_{12} +$$
$$+ Q_x^0\left(\Psi_x - \theta_1\right) + Q_y^0\left(\Psi_y - \theta_2\right) - 2qW\Big\}dxdy =$$
$$= \frac{Eh}{2\left(1-\mu^2\right)}\int_0^a\int_0^b \Big\{ \varepsilon_x^2 + 2\mu\varepsilon_y\varepsilon_x + \varepsilon_y^2 + \overline{G}_{12}\gamma_{xy}^2 + \frac{h^2}{12}\left(\chi_1^2 + 2\mu\chi_1\chi_2 + \chi_2^2 + 4\overline{G}_{12}\chi_{12}^2\right) + \quad (11)$$
$$+ \overline{G}_{13}k\left(\Psi_x - \theta_1\right)^2 + \overline{G}_{23}k\left(\Psi_y - \theta_2\right)^2 - \frac{2\left(1-\mu^2\right)qW}{Eh}\Big\}dxdy,$$
$$\overline{G}_{12} = \frac{G_{12}\left(1-\mu^2\right)}{E}, \overline{G}_{13} = \frac{G_{13}\left(1-\mu^2\right)}{E}, \overline{G}_{23} = \frac{G_{23}\left(1-\mu^2\right)}{E},$$

An expression for E_p^R is obtained analogously:

$$E_p^R = \frac{1}{2}\int_0^a\int_0^b \Big\{ N_x^R\varepsilon_x + N_y^R\varepsilon_y + \frac{1}{2}\left(N_{xy}^R + N_{yx}^R\right)\gamma_{xy} + M_x^R\chi_1 + M_y^R\chi_2 + \left(M_{xy}^R + M_{yx}^R\right)\chi_{12} +$$
$$+ Q_x^R\left(\Psi_x - \theta_1\right) + Q_y^R\left(\Psi_y - \theta_2\right)\Big\}dxdy =$$
$$= \frac{E}{2\left(1-\mu^2\right)}\int_0^a\int_0^b \Big\{\Big[F\left(\varepsilon_x^2 + 2\mu\varepsilon_y\varepsilon_x + \varepsilon_y^2 + \overline{G}_{12}\gamma_{xy}^2 + \overline{G}_{13}k\left(\Psi_x - \theta_1\right)^2 + \overline{G}_{23}k\left(\Psi_y - \theta_2\right)^2\right) + \quad (12)$$
$$+ 2\overline{S}\left(\varepsilon_x\chi_1 + \mu\varepsilon_y\chi_1 + \varepsilon_y\chi_2 + \mu\varepsilon_x\chi_2 + 2\overline{G}_{12}\gamma_{xy}\chi_{12}\right) + J\left(\chi_1^2 + \chi_2^2 + 2\mu\chi_1\chi_2 + 4\chi_{12}^2\right)\Big]\Big\}dxdy.$$

Algorithm

In this paper, it is proposed to use an algorithm based on the Ritz method and the method of parameter continuation for the study of shell structures.

According to this algorithm, the Ritz method is applied to the functional in order to reduce the variational problem to a system of nonlinear algebraic equations. For this, the required functions are represented in the form

$$U(x,y) = \sum_{I=1}^{N} U(I)Z1(I);\ V(x,y) = \sum_{I=1}^{N} V(I)Z2(I);\ W(x,y) = \sum_{I=1}^{N} W(I)Z3(I);$$
$$\Psi_x(x,y) = \sum_{I=1}^{N} PS(I)Z4(I);\ \Psi_y(x,y) = \sum_{I=1}^{N} PN(I)Z5(I), \quad (13)$$

and the system of nonlinear algebraic equations is obtained relative to the unknown numerical parameters $U(I)$, $V(I)$, $W(I)$, $PS(I)$, and $PN(I)$.

The convergence of the Ritz method in solving the problems of stability of thin-walled reinforced shells was shown in [40], where for problems with symmetric shells the difference in the critical load values for $N = 9$ and $N = 16$ was minimal. In this paper, all the results were obtained with $N = 9$.

Various numerical methods can be used to solve this system [40, 42, 43]. In this paper we use the parameter continuation method [40].

Approximation functions in (13) are selected depending on the method of fixing the shell contour, and must satisfy the boundary conditions. With the fixed-pin joint along the contour, we obtain the following boundary conditions:

for $x = 0,\ x = a$:

$$U = V = W = 0,\ \ M_x = 0,\ \ \Psi_y = 0;$$

for $y = 0,\ y = b$:

$$U = V = W = 0,\ \ M_y = 0,\ \ \Psi_x = 0.$$

Taking into account the fact that shallow shells of double curvature of square base have symmetry, the approximation functions for this type of fastening can be taken in the form:

$$U(x,y) = \sum_{k=1}^{\sqrt{N}}\sum_{l=1}^{\sqrt{N}} U_{kl} \sin\left(2k\pi\frac{x}{a}\right)\sin\left((2l-1)\pi\frac{y}{b}\right),$$

$$V(x,y) = \sum_{k=1}^{\sqrt{N}}\sum_{l=1}^{\sqrt{N}} V_{kl} \sin\left((2k-1)\pi\frac{x}{a}\right)\sin\left(2l\pi\frac{y}{b}\right),$$

$$W(x,y) = \sum_{k=1}^{\sqrt{N}}\sum_{l=1}^{\sqrt{N}} W_{kl} \sin\left((2k-1)\pi\frac{x}{a}\right)\sin\left((2l-1)\pi\frac{y}{b}\right),$$

$$\Psi_x(x,y) = \sum_{k=1}^{\sqrt{N}}\sum_{l=1}^{\sqrt{N}} PS_{kl} \cos\left((2k-1)\pi\frac{x}{a}\right)\sin\left((2l-1)\pi\frac{y}{b}\right),$$

$$\Psi_y(x,y) = \sum_{k=1}^{\sqrt{N}}\sum_{l=1}^{\sqrt{N}} PN_{kl} \sin\left((2k-1)\pi\frac{x}{a}\right)\cos\left((2l-1)\pi\frac{y}{b}\right).$$

Results and Discussion

Calculations are carried out for shallow shells of double curvature of square base with $a = b$, and $R_1 = R_2$, with fixed-pin joint along the contour and subjected to uniformly distributed transverse loading.

Let us introduce the dimensionless parameters

$$\xi = \frac{x}{a},\ \eta = \frac{y}{b},\ \overline{U} = \frac{aU}{h^2},\ \overline{V} = \frac{bV}{h^2},\ \overline{W} = \frac{W}{h},\ k_\xi = \frac{a^2 k_x}{h},\ k_\eta = \frac{b^2 k_y}{h},\ \Psi_x = \frac{a\Psi_x}{h},$$
$$\Psi_y = \frac{b\Psi_y}{h},\ \overline{P} = \frac{a^4 q}{Eh^4},\quad \sigma_\eta = \frac{a^2\sigma_y}{Eh^2},\ \ N_\eta = \frac{a^2 N_y}{Eh^3}, M_\eta = \frac{a^2 M_y}{Eh^4}, \tag{14}$$

We will investigate the nature of stress distribution on the outer surface of the shells for different numbers of shell-reinforcing stiffeners with height $3h$ and width $2h$ for a=60h and $R_1 = R_2 = 225h$ $\left(k_\xi = k_\eta = 16\right)$.

Figure 2 shows the stress diagrams σ_η for $\overline{P} = 150,$ reinforced with four stiffeners (Figure 2, a) and two stiffeners (Figure 2, b). The curve with number 1 corresponds to the cross-section $\xi = 0.1,$ curve 2 to the cross-section $\xi = 0.2,$ curve 3 to the cross-section $\xi = 0.3,$ curve 4 to the cross-section $\xi = 0.4,$ and curve 5 to the cross-section $\xi = 0.5.$

As can be seen from Figure 2, the stresses on the stiffener decrease substantially, but closer to the central cross-section $(\xi = 0.5)$, the character of the stress becomes smoother.

For shells reinforced with two wide stiffeners (width $12h$), the stress pattern remains the same (Figure 2, c).

Now let us investigate the nature of the distribution of forces and moments in the stiffeners and in the shell skin.

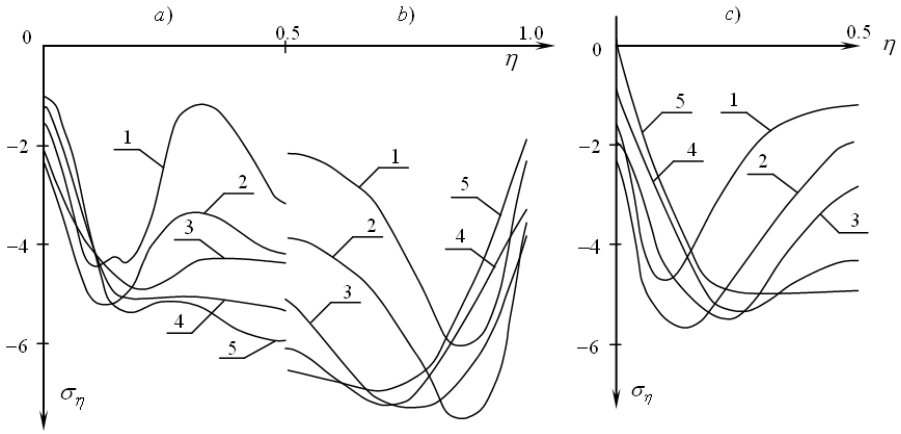

Figure 2. Diagram of stresses σ_η of a shallow shell with various cross-sections

Figure 3 shows diagrams of forces N_η^R and moments M_η^R acting in the stiffener (Figure 3, a) and along the stiffener (Figure 3, b); and N_η^0 and M_η^0 (Figures 3, c and 3, d) in the shell skin along the stiffener (for the shell reinforced by two stiffeners intersecting in the center with height $3h$ and various widths for $\bar{P}$=150, ξ=0.5).

Curve 1 corresponds to the width of the stiffener $2h$, curve 2 to width $12h$, and curve 3 to width $24h$. As can be seen from Figure 3, the forces and moments in the cross-section of the stiffener are much larger than in the shell skin. Moreover, the fibers in the shell skin are compressed, and the fibers in the stiffener are elongated, because N_η^R and N_η^0 have opposite signs.

Figures 3,e and 3,f show the diagrams of moments M_η^0 and forces N_η^0 in the cross-section of a shell skin $\eta = 0.1$ (between the stiffeners). All values presented in Figure 3 are related to the unit length of the cross-section.

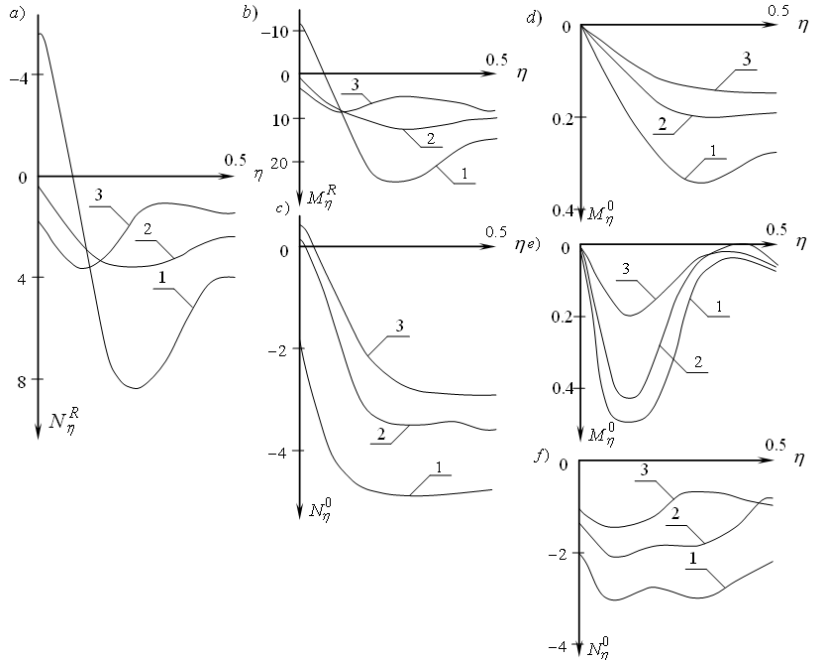

Figure 3. Diagrams of forces N_η and moments M_η of a shallow shell in the cross-section $\xi = 0.5$

Карпов В.В., Игнатьев О.В., Семенов А.А. Напряженно-деформированное состояние ребристых оболочечных конструкций // Инженерно-строительный журнал. 2017. № 6(74). С. 147-160.

As can be seen from Figure 3, as the width of the stiffener decreases, the forces and moments in the stiffeners increase. Let us consider shells reinforced with two and four intersecting stiffeners of height $3h$ and width h. In Figures 4 and 5, the curve number indicates the number of shell-reinforcing stiffeners.

Figure 4 shows the "load $\overline{P}$ - deflection $\overline{W}$ in the center of the shell" dependencies and diagrams of the angles of rotation of the normal Ψ_x along the axis ξ for $\overline{P}=150$ and $\eta=0.1$. As can be seen from this figure, at the point where the stiffener is attached to the shell skin, the angles of rotation Ψ_x become practically equal to zero.

Figure 5 shows the diagrams of forces N_η^R (Figure 5, a) and N_η^0 (Figure 5, b), and moments M_η^R (Figure 5, c) and M_η^0 (Figure 5, d) per unit length of the cross-section, for $\overline{P}=150$ along the stiffener (parallel to the *y* axis).

Since the force and moment diagrams are given along the stiffener, then for the shells reinforced with two stiffeners, the stiffener is located at $\xi=0.5$, and for the shells reinforced with four stiffeners at $\xi=0.35$.

As can be seen from Figure 5, in the cross section of the stiffener, significant forces and moments appear along the stiffener, while these values are much smaller in the shell skin. Near the edge, the stiffener is subject to compression, and further from the edge, to elongation. At the place of intersection of the stiffeners, the forces are reduced. A smooth change in the forces is observed in the shell skin.

Since the model of the stiffened shell, taking into account the transverse shears, permits the out-of-plane bending of the stiffener, let us analyze this point.

Figure 6 shows the diagrams of bending moments M_η^R (in the direction of the axis η) in the cross-section of the stiffener $(\xi=0.5)$ and the longitudinal section of the stiffener $(\eta=0.5)$ which are mutually orthogonal, for the shells reinforced with a different number of stiffeners: 2 stiffeners (curve 2) and 6 stiffeners (curve 6), with height 3*h* and width *h*. The index “1” in Figure 6 designates that the height of the stiffeners is $6h$ and the width is h. A shallow shell of square base with parameters $a=120h,\ k_\xi=32$ is subject to uniformly distributed transverse loading, $\overline{P}=500$.

As can be seen from Figure 6, the bending of a stiffener in cross-section is somewhat larger than in longitudinal section, but is of the same order. As the height of the stiffener increases, bending moments also increase. At the intersections of the stiffeners, their bending (out-of-plane) decreases. The direction of bending of the stiffener out of its plane differs for a shell that has only one stiffener in the direction being examined and a shell that has several stiffeners in the direction being examined.

Next, let us study the character of the normal stress distribution along the stiffener in different layers of the stiffened shell along the thickness of the stiffener.

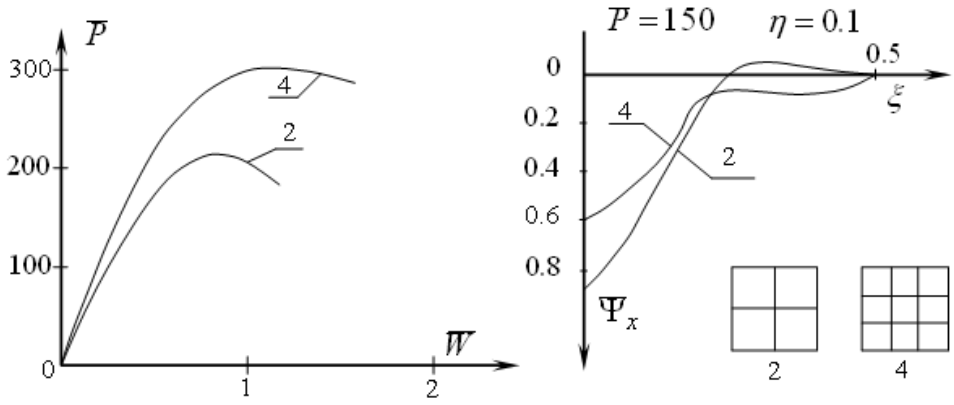

Figure 4. "Load-deflection" graphs for a shallow shell reinforced with two and four stiffeners, and diagrams of the angles of rotation of the normal $\overline{\Psi}_x$

Karpov V.V., Ignat’ev O.V., Semenov A.A. The stress-strain state of ribbed shell structures. *Magazine of Civil Engineering*. 2017. No. 6. Pp. 147–160. doi: 10.18720/MCE.74.12.

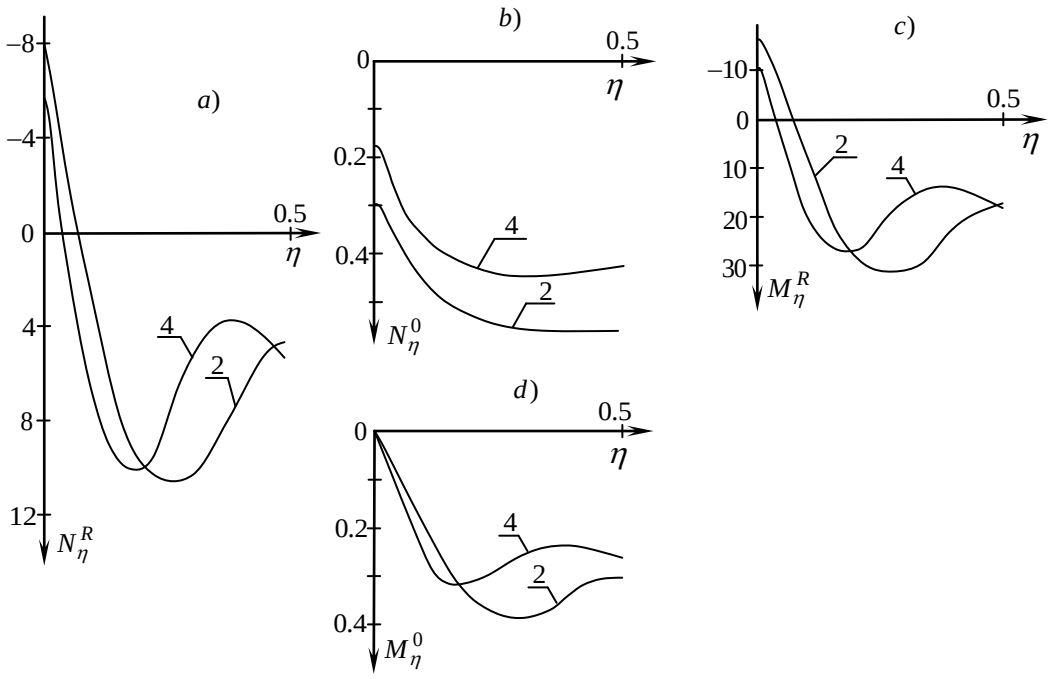

Figure 5. Diagrams of forces and moments in the shell skin and in the stiffeners of a shallow shell reinforced with two and four stiffeners

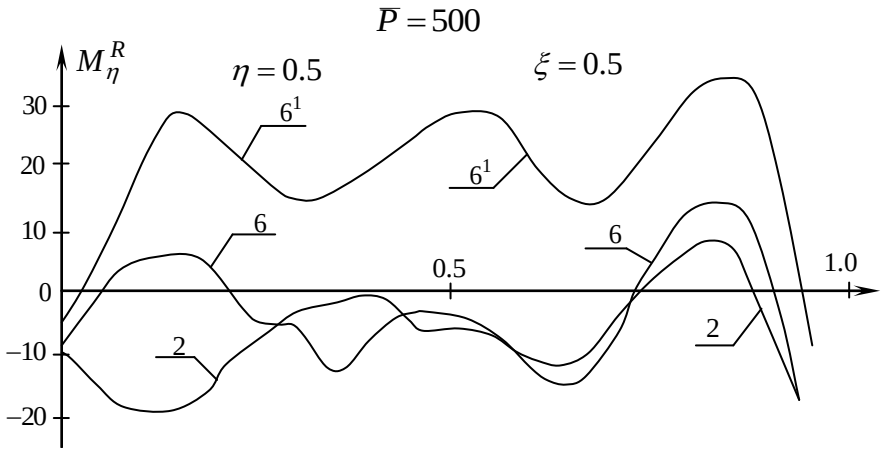

Figure 6. Diagrams of moments M_η^R in different cross-sections for a shallow shell reinforced with a different number of stiffeners

Let us examine the stress distribution in the shell skin and in the stiffener under critical load. Figure 7 shows the stress diagrams σ_η for $\xi = 0.5$ along the η axis for the shell with $a = 60h, k_\xi = 16$: curve 1 for $z = -h/2$, curve 2 for $z = 0$, curve 3 for $z = h/2$, curve 4 for $z = h/2 + 3h$ (at the center of the stiffener), and curve 5 for $z = h/2 + 6h$ (bottom part of the stiffener). Figure 8 shows similar results for shells with parameters $k_\xi = 32$, $a = 120h$ (index "1"), and $a = 240h$ (index "2") near the critical load value (for the shell with $a = 120h$, $\bar{P}_{kr} = 1860$, and for the shell with $a = 240h$, $\bar{P}_{kr} = 1580$). The shells are reinforced with six stiffeners with height $3h$ and width $2h$.

Карпов В.В., Игнатьев О.В., Семенов А.А. Напряженно-деформированное состояние ребристых оболочечных конструкций // Инженерно-строительный журнал. 2017. № 6(74). С. 147-160.

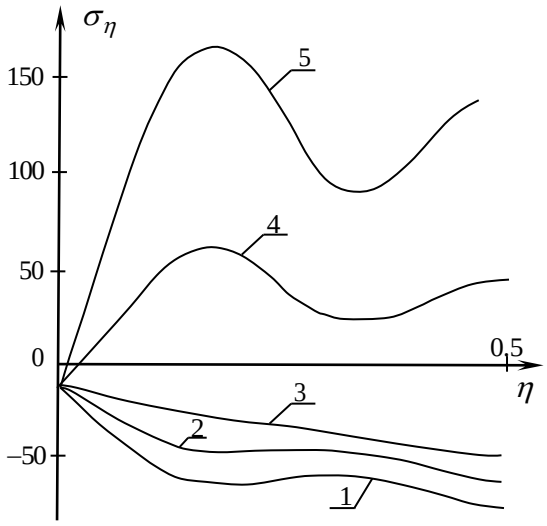

Figure 7. Diagram of stresses σ_η in different cross-sections of the stiffener for $a = 60h, k_\xi = 16$

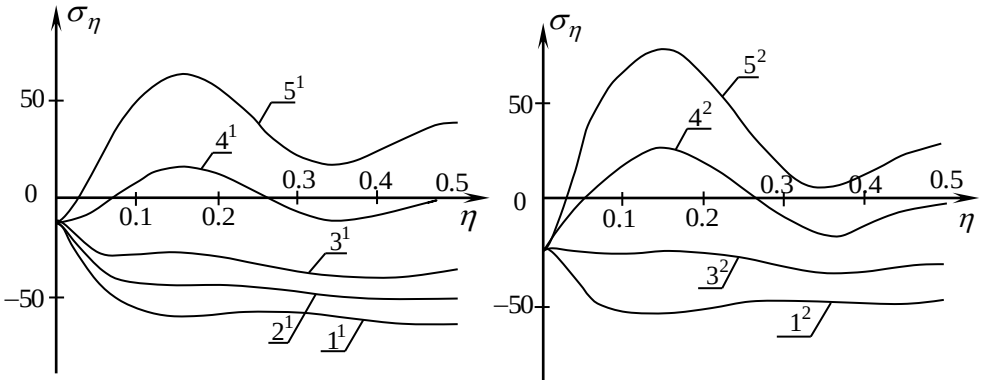

Figure 8. Diagram of stresses σ_η in different cross-sections of the stiffener for $a = 120h, k_\xi = 32$

As can be seen from Figures 7 and 8, stresses occurring in the stiffener significantly exceed stresses in the shell skin. These stresses increase with the height of the stiffener. Therefore, plastic deformations will appear in the stiffener first, and only afterwards in the shell skin. When plastic deformations occur in the stiffener, the moment of stability loss may occur earlier.

Therefore, it is necessary to analyze the maximum stresses in the shell and stiffeners for comparison with the maximum allowable values in order to remain in the elastic zone.

To confirm the reliability of this approach to the introduction of stiffeners, let us consider the results of an experimental study of the stability of stiffened shells, performed at the Ural Scientific Center of the USSR Academy of Sciences and described in the work of V. I. Klimanov and S. A. Timashev [43]. Tests were carried out on 18 samples of shallow shells of square base from plexiglass, the parameters of which are $a = b = 0.6$ m, $R_1 = R_2 = 1.51$ m, $h = 0.001$ m, reinforced by an orthogonal grid of stiffeners with a cross-sectional area 0.0033×0.0092 m² ($3.3h \times 9.2h$) and step size for stiffener arrangement 0.075 m (9×9 stiffeners). The dimensionless parameters of the curvature of such shells are $k_\xi = k_\eta = 238$. The load was assumed to be uniformly distributed over the area of the shell.

As a result of the experiment, the authors of Ref. [43] obtained critical load values that ranged from $0.411 \cdot 10^{-2}$ MPa to $0.703 \cdot 10^{-2}$ MPa. According to the method of calculation of reinforced shells proposed by us, a study of similar structure was conducted: when reinforced with stiffeners ($3.3h \times 9.2h$), the critical load value is $0.72 \cdot 10^{-2}$ MPa (the difference in values is explained by the fact that during calculations, the ideal structure is considered, as well as the possibility of plastic deformations and other factors), and when reinforced with stiffeners ($2h \times 3h$) the critical load value is $0.3 \cdot 10^{-2}$ MPa.

Karpov V.V., Ignat'ev O.V., Semenov A.A. The stress-strain state of ribbed shell structures. *Magazine of Civil Engineering*. 2017. No. 6. Pp. 147–160. doi: 10.18720/MCE.74.12.

It is also noted in [43] that the shells were initially exposed to cavities, which, under further loading, developed to a depth of $0.55h$. On average, under load $q = 0.195 \cdot 10^{-2}$ MPa, deflections of the model centers are $2.5h$. For a load $q = 0.389 \cdot 10^{-2}$ MPa, they were equal to $7h$ [43]. Similar qualitative results of the process of stability loss of the shell were obtained in this work.

Conclusions

As a result of the calculations and analysis of the data obtained, the following features of the stress-strain state of stiffened shallow shell structures of double curvature can be outlined:

- when the shell is reinforced with a small number of stiffeners, stresses in the area of their connection to the shell skin decrease quickly, and their redistribution occurs in comparison with the smooth shell, but closer to the central cross-section $(\xi = 0.5)$ the character of stresses becomes smoother. Moreover, as the width of the stiffeners increases, the nature of the stresses remains the same;
- as the number of stiffeners increases, the distribution of stresses on the outer surface of the shell skin becomes smoother;
- as the width of the stiffener decreases, the forces and moments in the stiffeners increase;
- at the places where the stiffeners are connected to the shell skin, the angles of rotation of the normal Ψ_x become close to zero, but in the other part of the shell they increase, so that, in comparison with smooth shells, accounting for transverse shears significantly affects the stress-strain state of the stiffened shell;
- in the cross-section of the stiffener there are significant forces and moments, whereas in the shell skin these values are much less than in the stiffener itself. Near the contour of the shell, the stiffener is subject to compression, and closer to the center it is under tension.
- as the height of the stiffener increases, bending moments in the stiffener increase;
- at the intersection of the stiffeners, their bending (out of the plane of the stiffener) decreases, which proves the necessity to take into account the joint action of the stiffeners at their intersection. With the introduction of stiffeners along the line, this effect is not taken into account;
- stresses occurring in the stiffener significantly exceed stresses in the shell skin. These stresses increase with the height of the stiffener. Therefore, plastic deformations will occur first in the stiffener, and then in the shell skin. When plastic deformations develop in the stiffener, the moment of stability loss may occur earlier.

Thus, taking into account the contact of the stiffener with the shell skin along the strip makes it possible to investigate the stress-strain state in the stiffeners, which is not possible using delta functions with the introduction of stiffeners along the line.

Reference

1. Smerdov A.A. A computational study in optimum formulations of optimization problems on laminated cylindrical shells for buckling II. Shells under external pressure. *Composites Science and Technology.* 2000. Vol. 60. No. 11. Pp. 2067–2076.
2. Lutskaya I.V., Maksimyuk V.A., Storozhuk E.A., Chernyshenko I.S. Nonlinear elastic deformation of thin composite shells of discretely variable thickness. *International Applied Mechanics.* 2016. Vol. 52. No. 6. Pp. 616–623.
3. Leonenko D.V., Starovoitov E.I. Vibrations of cylindrical sandwich shells with elastic core under local loads. *International Applied Mechanics.* 2016. Vol. 52. No. 4. Pp. 359–367.
4. Kopecki T., Święch Ł. Experimental and numerical analysis of post-buckling deformation states of integrally stiffened thin-walled components of load-bearing aircraft structures. *Journal of Theoretical and Applied Mechanics.* 2014.

Литература

1. Smerdov A.A. A computational study in optimum formulations of optimization problems on laminated cylindrical shells for buckling II. Shells under external pressure // Composites Science and Technology. 2000. Vol. 60. № 11. Pp. 2067–2076.
2. Lutskaya I.V., Maksimyuk V.A., Storozhuk E.A., Chernyshenko I.S. Nonlinear elastic deformation of thin composite shells of discretely variable thickness // International Applied Mechanics. 2016. Vol. 52. № 6. Pp. 616–623.
3. Leonenko D.V., Starovoitov E.I. Vibrations of cylindrical sandwich shells with elastic core under local loads // International Applied Mechanics. 2016. Vol. 52. № 4. Pp. 359–367.
4. Kopecki T., Święch Ł. Experimental and numerical analysis of post-buckling deformation states of integrally stiffened thin-walled components of load-bearing aircraft structures // Journal of Theoretical and Applied Mechanics. 2014.

Карпов В.В., Игнатьев О.В., Семенов А.А. Напряженно-деформированное состояние ребристых оболочечных конструкций // Инженерно-строительный журнал. 2017. № 6(74). С. 147-160.

Vol. 52. No. 4. Pp. 905–915.

5. Krivoshapko S.N. Research on General and Axisymmetric Ellipsoidal Shells Used as Domes, Pressure Vessels, and Tanks. *Applied Mechanics Reviews.* 2007. Vol. 60. No. 6. Pp. 336–355.
6. Kondratyeva L.N., Routman Y.L., Maslennikov A.M., Golykh O.V. Analytical Method of Determining Folded Depressed Shells Free Oscillation Frequency. *Advanced Materials Research.* 2014. Vol. 1020. Pp. 291–296.
7. Li D., Qing G., Liu Y. A layerwise/solid-element method for the composite stiffened laminated cylindrical shell structures. *Composite Structures.* 2013. Vol. 98. Pp. 215-227.
8. Shi P., Kapania R.K., Dong C. Free Vibration Analysis of Curvilinearly Stiffened Cylindrical Shells. American Institute of Aeronautics and Astronautics. *Proceedings of 56th AIAA/ASCE/AHS/ASC Structures, Structural Dynamics, and Materials Conference, AIAA SciTech Forum.* AIAA, 2015. Vols. 2015-2050. Pp. 1–19.
9. Garrido M., Correia J. R., Keller T., Cabral-Fonseca S. Creep of sandwich panels with longitudinal reinforcement ribs for civil engineering applications: experiments and composite creep modeling. *Journal of Composites for Construction.* 2017. Vol. 21. No. 1. Pp. 04016074.
10. Gavrilenko G.D., Matsner V.I. Experimental justification of the analytical method for determining the upper and lower bounds of the critical loads in ribbed shells. *Strength of Materials.* 2006. Vol. 38. No. 2. Pp. 150–165.
11. Wang B., Du K., Hao P., Zhou C., Tian K., Xu S., Ma Y., Zhang X. Numerically and experimentally predicted knockdown factors for stiffened shells under axial compression. *Thin-Walled Structures.* 2016. Vol. 109. Pp. 13–24.
12. Less H., Abramovich H. Dynamic buckling of a laminated composite stringer–stiffened cylindrical panel. *Composites Part B: Engineering.* 2012. Vol. 43. No. 5. Pp. 2348–2358.
13. Qu Y., Chen Y., Long X., Hua H., Meng G. A modified variational approach for vibration analysis of ring-stiffened conical–cylindrical shell combinations. *European Journal of Mechanics - A/Solids.* 2013. Vol. 37. Pp. 200–215.
14. Duc N.D. Corrigendum to “Nonlinear dynamic response of imperfect eccentrically stiffened FGM double curved shallow shells on elastic foundation” [Compos. Struct. 99 (2013) 88–96]. *Composite Structures.* 2013. Vol. 102. Pp. 306–314.
15. Bich D.H., Dung D.V., Nam V.H. Nonlinear dynamic analysis of eccentrically stiffened imperfect functionally graded doubly curved thin shallow shells. *Composite Structures.* 2013. Vol. 96. Pp. 384–395.
16. Dung D.V., Chan D.Q. Analytical investigation on mechanical buckling of FGM truncated conical shells reinforced by orthogonal stiffeners based on FSDT. *Composite Structures.* 2017. Vol. 159. Pp. 827–841.
17. Barlag S., Rothert H. An idealization concept for the stability analysis of ring-reinforced cylindrical shells under external pressure. *International Journal of Non-Linear Mechanics.* 2002. Vol. 37. No. 4–5. Pp. 745–756.
18. Dung D.V., Hoa L.K., Nga N.T., Anh L.T.N. Instability of eccentrically stiffened functionally graded truncated conical shells under mechanical loads. *Composite Structures.* 2013. Vol. 106. Pp. 104–113.
19. Patel S.N., Datta P.K., Sheikh A.H. Buckling and dynamic instability analysis of stiffened shell panels. *Thin-Walled Structures.* 2006. Vol. 44. No. 3. Pp. 321–333.
20. Hilburger M.W., Starnes Jr. J.H. Buckling behavior of compression-loaded composite cylindrical shells with reinforced cutouts. *International Journal of Non-Linear Mechanics.* 2005. Vol. 40. No. 7. Pp. 1005–1021.
21. Xiang Y., Wang C.M., Lim C.W., Kitipornchai S. Buckling of intermediate ring supported cylindrical shells under axial compression. *Thin-Walled Structures.* 2005. Vol. 43. No. 3. Pp. 427–443.

Vol. 52. № 4. P. 905–915.

5. Krivoshapko S.N. Research on general and axisymmetric ellipsoidal shells used as domes, pressure vessels, and tanks // Applied Mechanics Reviews. 2007. Vol. 60. № 6. Pp. 336–355.
6. Kondratyeva L.N., Routman Y.L., Maslennikov A.M., Golykh O.V. Analytical method of determining folded depressed shells free oscillation frequency // Advanced Materials Research. 2014. Vol. 1020. Pp. 291–296.
7. Li D., Qing G., Liu Y. A layerwise/solid-element method for the composite stiffened laminated cylindrical shell structures // Composite Structures. 2013. Vol. 98. Pp. 215–227.
8. Shi P., Kapania R.K., Dong C. Free vibration analysis of curvilinearly stiffened cylindrical shells. american institute of aeronautics and astronautics // Proceedings of 56th AIAA/ASCE/AHS/ASC Structures, Structural Dynamics, and Materials Conference, AIAA SciTech Forum. AIAA, 2015. Vols. 2015-2050. Pp. 1–19.
9. Garrido M., Correia J. R., Keller T., Cabral-Fonseca S. Creep of sandwich panels with longitudinal reinforcement ribs for civil engineering applications: experiments and composite creep modeling // Journal of Composites for Construction. 2017. Vol. 21. № 1. P. 04016074.
10. Gavrilenko G.D., Matsner V.I. Experimental justification of the analytical method for determining the upper and lower bounds of the critical loads in ribbed shells // Strength of Materials. 2006. Vol. 38. № 2. Pp. 150–165.
11. 11. Wang B., Du K., Hao P., Zhou C., Tian K., Xu S., Ma Y., Zhang X. Numerically and experimentally predicted knockdown factors for stiffened shells under axial compression // Thin-Walled Structures. 2016. Vol. 109. Pp. 13–24.
12. Less H., Abramovich H. Dynamic buckling of a laminated composite stringer–stiffened cylindrical panel // Composites Part B: Engineering. 2012. Vol. 43. № 5. Pp. 2348–2358.
13. Qu Y., Chen Y., Long X., Hua H., Meng G. A modified variational approach for vibration analysis of ring-stiffened conical–cylindrical shell combinations // European Journal of Mechanics - A/Solids. 2013. Vol. 37. Pp. 200–215.
14. Duc N.D. Corrigendum to “Nonlinear dynamic response of imperfect eccentrically stiffened FGM double curved shallow shells on elastic foundation” [Compos. Struct. 99 (2013) 88–96] // Composite Structures. 2013. Vol. 102. Pp. 306–314.
15. Bich D.H., Dung D.V., Nam V.H. Nonlinear dynamic analysis of eccentrically stiffened imperfect functionally graded doubly curved thin shallow shells // Composite Structures. 2013. Vol. 96. Pp. 384–395.
16. Dung D.V., Chan D.Q. Analytical investigation on mechanical buckling of FGM truncated conical shells reinforced by orthogonal stiffeners based on FSDT // Composite Structures. 2017. Vol. 159. Pp. 827–841.
17. Barlag S., Rothert H. An idealization concept for the stability analysis of ring-reinforced cylindrical shells under external pressure // International Journal of Non-Linear Mechanics. 2002. Vol. 37. № 4–5. Pp. 745–756.
18. Dung D.V., Hoa L.K., Nga N.T., Anh L.T.N. Instability of eccentrically stiffened functionally graded truncated conical shells under mechanical loads // Composite Structures. 2013. Vol. 106. Pp. 104–113.
19. Patel S.N., Datta P.K., Sheikh A.H. Buckling and dynamic instability analysis of stiffened shell panels // Thin-Walled Structures. 2006. Vol. 44. № 3. Pp. 321–333.
20. Hilburger M.W., Starnes Jr. J.H. Buckling behavior of compression-loaded composite cylindrical shells with reinforced cutouts // International Journal of Non-Linear Mechanics. 2005. Vol. 40. № 7. Pp. 1005–1021.
21. Xiang Y., Wang C.M., Lim C.W., Kitipornchai S. Buckling of intermediate ring supported cylindrical shells under axial compression // Thin-Walled Structures. 2005. Vol. 43. № 3. Pp. 427–443.
22. Mouhat O., Khamlichi A. Effect of loading pulse duration on

Karpov V.V., Ignat’ev O.V., Semenov A.A. The stress-strain state of ribbed shell structures. *Magazine of Civil Engineering*. 2017. No. 6. Pp. 147–160. doi: 10.18720/MCE.74.12.

22. Mouhat O., Khamlichi A. Effect of loading pulse duration on dynamic buckling of stiffened panels. *MATEC Web of Conferences.* 2014. Vol. 16. Pp. 07006.
23. Dung D.V., Dong D.T. Nonlinear thermo-mechanical stability of eccentrically stiffened functionally graded material sandwich doubly curved shallow shells with general sigmoid law and power law according to third-order shear deformation theory. *Applied Mathematics and Mechanics.* 2017. Vol. 38. No. 2. Pp. 191–216.
24. Weber M.J., Middendorf P. Semi-analytical skin buckling of curved orthotropic grid-stiffened shells. *Composite Structures.* 2014. Vol. 108. Pp. 616–624.
25. Qu Y., Wu S., Chen Y., Hua H. Vibration analysis of ring-stiffened conical–cylindrical–spherical shells based on a modified variational approach. *International Journal of Mechanical Sciences.* 2013. Vol. 69. Pp. 72–84.
26. Siryus V. Minimization of the weight of ribbed cylindrical shells made of a viscoelastic composite. *Mechanics of Composite Materials.* 2011. Vol. 46. No. 6. Pp. 593–598.
27. Jarmai K., Snyman J.A., Farkas J. Minimum cost design of a welded orthogonally stiffened cylindrical shell. *Computers & Structures.* 2006. Vol. 84. No. 12. Pp. 787–797.
28. Simões L.M.C., Farkas J., Jármai K. Reliability-based optimum design of a welded stringer-stiffened steel cylindrical shell subject to axial compression and bending. *Structural and Multidisciplinary Optimization.* 2006. Vol. 31. No. 2. Pp. 147–155.
29. Hao P., Wang B., Tian K., Liu H., Wang Y., Niu F., Zeng D. Simultaneous buckling design of stiffened shells with multiple cutouts. *Engineering Optimization.* 2017. Vol. 49. No. 7. Pp. 1116–1132.
30. Lene F., Duvaut G., Olivier-Mailhe M., Ben Chaabane S., Grihon S. An advanced methodology for optimum design of a composite stiffened cylinder. *Composite Structures*. 2009. Vol. 91. No. 4. Pp. 392–397.
31. Yu W., Li Z.L. Structural Similitude for Prestressed Vibration and Buckling of Eccentrically Stiffened Circular Cylindrical Panels and Shells by Energy Approach. *International Journal of Structural Stability and Dynamics.* 2016. Vol. 16. No. 10. Pp. 1550074.
32. Abramovich H., Zarutskii V.A. Effect of the stiffness of ribs on the vibrations and stability of open cylindrical shells. *International Applied Mechanics*. 2011. Vol. 46. No. 9. Pp. 994–1000.
33. Amiro I.Ya., Zarutskii V.A. *Metody rascheta obolochek. Tom 2. Teoriya rebristykh obolochek* [Theory of Ribbed Shells, Vol. 2 of the five-volume series Methods of Shell Design]. Kiev: Naukova Dumka, 1980. 368 p. (rus)
34. Fialko S.Yu., Ankyaniec E.K. Vibrations of thin cylindrical shells with non-stiff connection between ribs and panelling. *Proceedings of the 8th SSTA Conference*, Jurata, Poland, 12-14 October 2005. Shell Structures: Theory and Applications. Pp. 315–318.
35. Fialko S.Y. Stress–strain analysis of thin-walled shells with massive ribs. *International Applied Mechanics.* 2004. Vol. 40. No. 4. Pp. 432–439.
36. Lurye A.I. *Obshchiye uravneniya obolochki, podkreplennoy rebrami zhestkosti* [General equations of the shell, reinforced by stiffeners]. Leningrad, 1948. 28 p. (rus)
37. Vlasov V.Z. *Kontaktnyye zadachi po teorii obolochek i tonkostennykh sterzhney* [Contact problems on the theory of shells and thin-walled rods]. Izv. AN SSSR. OTN. 1949. No. 6. Pp. 819–939. (rus)
38. Karmishin A.V., Lyaskovets V.A, Myachenkov V.I., Frolov A.N. *Statika i dinamika tonkostennykh obolochechnykh konstruktsiy* [Statics and dynamics of thin-walled shell structures]. Moscow: Mashinostroyeniye, 1975. 376 p. (rus)
39. Karpov V.V., Ignatyev O.V., Salnikov A.Yu. *Nelineynyye matematicheskiye modeli deformirovaniya obolochek peremennoy tolshchiny i algoritmy ikh issledovaniya* dynamic buckling of stiffened panels // MATEC Web of Conferences / ed. Belhaq M. 2014. Vol. 16. P. 07006.
23. Dung D.V., Dong D.T. Nonlinear thermo-mechanical stability of eccentrically stiffened functionally graded material sandwich doubly curved shallow shells with general sigmoid law and power law according to third-order shear deformation theory // Applied Mathematics and Mechanics. 2017. Vol. 38. № 2. Pp. 191–216.
24. Weber M.J., Middendorf P. Semi-analytical skin buckling of curved orthotropic grid-stiffened shells // Composite Structures. 2014. Vol. 108. P. 616–624.
25. Qu Y., Wu S., Chen Y., Hua H. Vibration analysis of ring-stiffened conical–cylindrical–spherical shells based on a modified variational approach // International Journal of Mechanical Sciences. 2013. Vol. 69. Pp. 72–84.
26. Siryus V. Minimization of the weight of ribbed cylindrical shells made of a viscoelastic composite // Mechanics of Composite Materials. 2011. Vol. 46. № 6. Pp. 593–598.
27. Jarmai K., Snyman J.A., Farkas J. Minimum cost design of a welded orthogonally stiffened cylindrical shell // Computers & Structures. 2006. Vol. 84. № 12. Pp. 787–797.
28. Simões L.M.C., Farkas J., Jármai K. Reliability-based optimum design of a welded stringer-stiffened steel cylindrical shell subject to axial compression and bending // Structural and Multidisciplinary Optimization. 2006. Vol. 31, № 2. P. 147–155.
29. Hao P., Wang B., Tian K., Liu H., Wang Y., Niu F., Zeng D. Simultaneous buckling design of stiffened shells with multiple cutouts // Engineering Optimization. 2017. Vol. 49. № 7. Pp. 1116–1132.
30. Lene F., Duvaut G., Olivier-Mailhe M., Ben Chaabane S., Grihon S. An advanced methodology for optimum design of a composite stiffened cylinder // Composite Structures. 2009. Vol. 91. № 4. Pp. 392–397.
31. Yu W., Li Z.L. Structural Similitude for Prestressed Vibration and Buckling of Eccentrically Stiffened Circular Cylindrical Panels and Shells by Energy Approach // International Journal of Structural Stability and Dynamics. 2016. Vol. 16. № 10. P. 1550074.
32. Abramovich H., Zarutskii V.A. Effect of the stiffness of ribs on the vibrations and stability of open cylindrical shells // International Applied Mechanics. 2011. Vol. 46. № 9. Pp. 994–1000.
33. Амиро И.Я., Заруцкий В.А. Методы расчета оболочек. Том 2. Теория ребристых оболочек. Киев: Наукова думка, 1980. 368 с.
34. Fialko S.Yu., Ankyaniec E.K. Vibrations of thin cylindrical shells with non-stiff connection between ribs and paneling // Proceedings of the 8th SSTA Conference, Jurata, Poland, 12-14 October 2005. Shell Structures: Theory and Applications. Pp. 315–318.
35. Fialko S.Y. Stress–strain analysis of thin-walled shells with massive ribs // International Applied Mechanics. 2004. Vol. 40. № 4. Pp. 432–439.
36. Лурье А.И. Общие уравнения оболочки, подкрепленной ребрами жесткости. Ленинград, 1948. 28 с.
37. Власов В.З. Контактные задачи по теории оболочек и тонкостенных стержней // Изв. АН СССР. ОТН. 1949. № 6. С. 819–939.
38. Кармишин А.В., Лясковец В.А, Мяченков В.И., Фролов А.Н. Статика и динамика тонкостенных оболочечных конструкций. М.: Машиностроение, 1975. 376 с.
39. Карпов В.В., Игнатьев О.В., Сальников А.Ю. Нелинейные математические модели деформирования оболочек переменной толщины и алгоритмы их исследования. М.: Изд-во АСВ; СПб.: СПбГАСУ, 2002. 420 с.
40. Карпов В.В. Прочность и устойчивость подкрепленных оболочек вращения: в 2 ч. Ч.2: Вычислительный эксперимент при статическом механическом

[Nonlinear mathematical models of deformation of shells of variable thickness and algorithms for their investigation]. Moscow: Izd-vo ASV; Saint-Petersburg: SPbGASU, 2002. 420 p. (rus)

40. Karpov V.V. *Prochnost i ustoychivost podkreplennykh obolochek vrashcheniya: v 2 ch. Ch.2: Vychislitelnyy eksperiment pri staticheskom mekhanicheskom vozdeystvii* [Strength and stability of reinforced shells of rotation: in 2 parts. Part 2: Computational experiment with static mechanical action]. Moscow: Fizmatlit, 2011. 248 p. (rus)
41. Trushin S. Numerical algorithm for solving of nonlinear problems of structural mechanics based on the continuation method in combination with the dynamic relaxation method. *MATEC Web of Conferences.* 2016. Vol. 86. Pp. 01006.
42. Kuznetsov E.B., Leonov S.S. Parametrization of the Cauchy Problem for Systems of Ordinary Differential Equations with Limiting Singular Points. *Computational Mathematics and Mathematical Physics.* 2017. Vol. 57. No. 6. Pp. 931–952.
43. Klimanov V.I., Timashev S.A. *Nelineynyye zadachi podkreplennykh obolochek* [Nonlinear problems of supported shells]. Sverdlovsk: UNTs AN SSSR, 1985. 291 p. (rus)

воздействии. М: Физматлит, 2011. 248 с.

41. Trushin S. Numerical algorithm for solving of nonlinear problems of structural mechanics based on the continuation method in combination with the dynamic relaxation method // MATEC Web of Conferences. 2016. Vol. 86. P. 01006.
42. Kuznetsov E.B., Leonov S.S. Parametrization of the Cauchy Problem for Systems of Ordinary Differential Equations with Limiting Singular Points // Computational Mathematics and Mathematical Physics. 2017. Vol. 57. № 6. Pp. 931–952.
43. Климанов В.И., Тимашев С.А. Нелинейные задачи подкрепленных оболочек. Свердловск: УНЦ АН СССР, 1985. 291 с.

Vladimir Karpov,
vvkarpov@lan.spbgasu.ru

Oleg Ignat'ev,
ignatiev.oleg.v@yandex.ru

Alexey Semenov,
+7(812)5750549; sw.semenov@gmail.com

Владимир Васильевич Карпов,
эл. почта: vvkarpov@lan.spbgasu.ru

Олег Владимирович Игнатьев,
эл. почта: ignatiev.oleg.v@yandex.ru

Алексей Александрович Семенов,
+7(812)5750549;
эл. почта: sw.semenov@gmail.com

Karpov V.V., Ignat'ev O.V., Semenov A.A. The stress-strain state of ribbed shell structures. *Magazine of Civil Engineering*. 2017. No. 6. Pp. 147–160. doi: 10.18720/MCE.74.12.